NUCLEAR THEORY, Vol. 35 (2016)
eds. M. Gaidarov, N. Minkov, Heron Press, Sofia

Short Range Correlations in Nuclei – Progress and Prospects

D.B. Day[1]

[1]University of Virginia, Charlottesville, Virginia 22904

Abstract. Short-range correlations (SRCs) in nuclei, an area of longstanding study both theoretically and experimentally, are an aspect of nuclear structure that goes beyond the independent particle model. Short distance interactions between nucleons give rise to high momentum components common to all nuclei and arise from both the repulsive core of the NN potential and from tensor interactions. Evidence for SRCs and their isospin dependence has been well established and linked to the EMC effect though a fundamental understanding is lacking. A series of future experiments are planned.

1 Introduction

In the independent-particle shell model nucleons move in an average field, or potential, generated by the entire nucleus and two-body interactions are absent as are correlations in the ground state. This mean field approach implies long mean free paths and gives rise to a picture of protons and neutrons in nuclear shells akin to the standard picture of electrons in atomic shells. Notably, there are aspects of the nucleon-nucleon (NN) interaction that get imposed on nuclear wave functions and are beyond what can be generated by the independent particle model. A full understanding of the nuclear ground state must include correlations; both those due to the long range part of the interaction and which gives rise to mixing of the valence configurations and those due to the short-range part of the NN interaction which is singularly repulsive. This feature has significant implications: there is a loss of configuration space and the momentum distributions acquire a tail extending to very high momentum. Both the correlation hole and the high-k components are absent in IPSMs and, taken together, are referred to as short range correlations (SRCs). In addition an isospin dependence is linked to the tensor part of the potential. Electron scattering experiments have provided a wealth of information about the strength of SRCs via cross section ratios of heavy to light nuclei in A(e,e') [1,2] and there is irrefutable evidence for their isospin dependence from experiments with multi-body final states [3,4]. In addition, a remarkable relationship has been observed [5,6] between the strength of SRCs determined in quasi-elastic electron-nucleon kinematics and the size of the EMC effect in deep inelastic kinematics where scattering from quarks are predominant. SRCs have been the subject of intense interest [7–11].

2 Evidence for SRC in Nuclei

The notion of the nucleons as an independent particles moving in a mean field is not supported by the saturation of nuclear density [12]. Spectroscopic factors measured in A$(e, e'p)$ experiments at NIKHEF for valence orbitals in closed-shell nuclei agree with mean field theory only when scaled by about 0.65 [13]. It is understood that this discrepancy is due to the effect of both short and long range correlations. Short range correlations also reveal themselves in the nuclear momentum distributions where it is found that all nuclei share a similar shape at large momentum k [8,14]. See Figure 1. Momentum distributions are calculable for few-body systems and nuclear matter and at $k > k_F$ are dominated by two-nucleon short range correlations. This region is still a poorly understood part of nuclear structure even though a significant fraction of nucleons ($\approx$ 20%) are beyond the predictions of the IPSM.

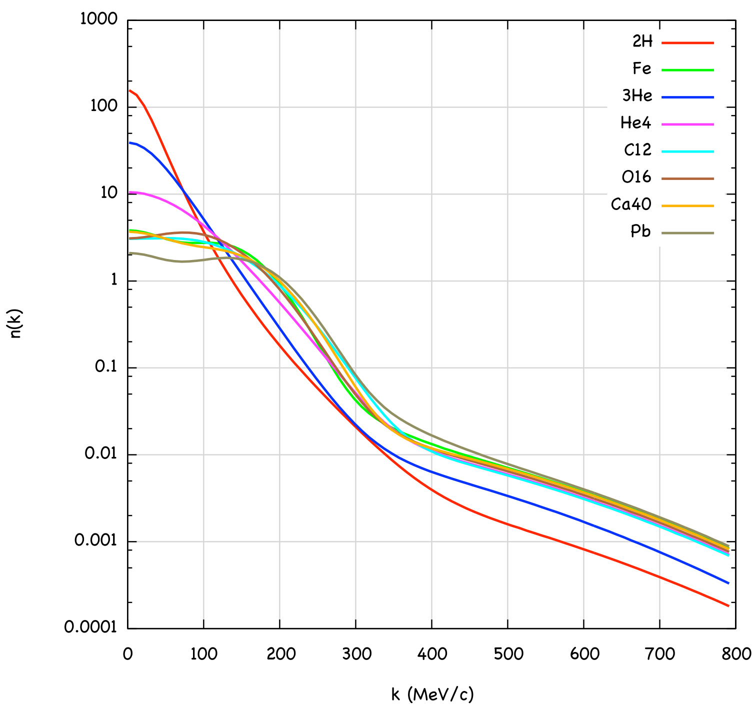

Figure 1. Theoretical nuclear momentum distributions for $n(k)$ a range of nuclei. Then field character is exposed at $k \leq 300$ MeV/c and that of the short range interactions at large k where all nuclei display a universal behavior. Figure based on momentum distributions found in Ref. [14].

3 Knockout Reactions

Knockout reactions are used to extract information about the ground state momentum and energy distributions. The incoming projectiles can be electrons, protons, or pions; electrons (the focus of this talk) have the advantage of being weakly interacting and can access the entire nuclear volume. Electrons are unlikely to undergo multistep interactions as do the strongly interacting probes. In both exclusive A(e,e'p) and inclusive A(e,e') processes the cross section can be written in term of the ground state momentum and energy distribution of the protons (and neutrons) encapsulated in the spectral function S(k,E) which gives the the joint probability to find in a nucleus a nucleon with momentum k and removal energy E: $d\sigma \propto \int d\vec{p} \int dES(k,E)\sigma_{ei}\delta()$. The cross section involves the integral of S(k,E) over both E and k weighted by the elementary scattering cross section from a moving nucleon, σ_{ei}, and constrained by an energy and momentum conserving delta function. The nuclear momentum distribution is $n(k) = 4\pi \int_{E_{\rm min}}^{\infty} S(k,E)dE$ where $E_{\rm min}$ is the minimum removal energy, the separation energy. The energy balance in the δ function includes the energy and momentum of the knocked out proton, that of the recoiling residual $(A-1)$ system and any excitation it might obtain. In exclusive (or semiexclusive) reactions a detailed picture of the ground state can be recreated yet they suffer from large FSI contributions and significantly lower scattering rates than inclusive ones. For a still relevant review of knockout reactions see Ref. [15].

3.1 Inclusive Electron Scattering

In inclusive scattering only the scattered particle is detected and the details of the ground state are integrated over. The dominant reactions are quasi-elastic in which a nucleon is knocked out of the nucleus, and deep inelastic scattering from quarks in the moving moving–the final state is indeterminate. The main reactions have identical initial states yet have quite dissimilar Q^2 dependencies. The quasi-elastic process falls at least as fast as the form factors of the nucleon $\sim (1/Q^4)$ while the DIS reaction has a much weaker dependence on Q^2, like that of the asymptotic process of deep inelastic scattering (DIS) from quarks. By taking advantage of kinematics (x and Q^2) one can essentially isolate one or the other. More than 60 years ago Czyz and Gottfried [16] proposed inclusive electron scattering to study correlations in nuclei, specifically pointing out the region below the quasi-elastic peak (at small energy loss and $x > 1$) to be especially fruitful.

Inclusive electron scattering spectra from nuclei have distinct features. At momentum transfers above 1 GeV/c^2 is dominated by a broad quasi-elastic peak (QEP) located at an energy loss that corresponds to scattering from a free nucleon, $\nu = (e - e') = q^2/(2m_N)$ where q is the magnitude of the three-momentum transfer. A useful variable to determine the dominant reaction in the kinematics is $x = Q^2/2m_N\nu$ where $Q^2 = 4ee' \sin(\theta/2)^2$, the four momentum transfer. The quasi-elastic peak is at $x = 1$, deep inelastic scattering at

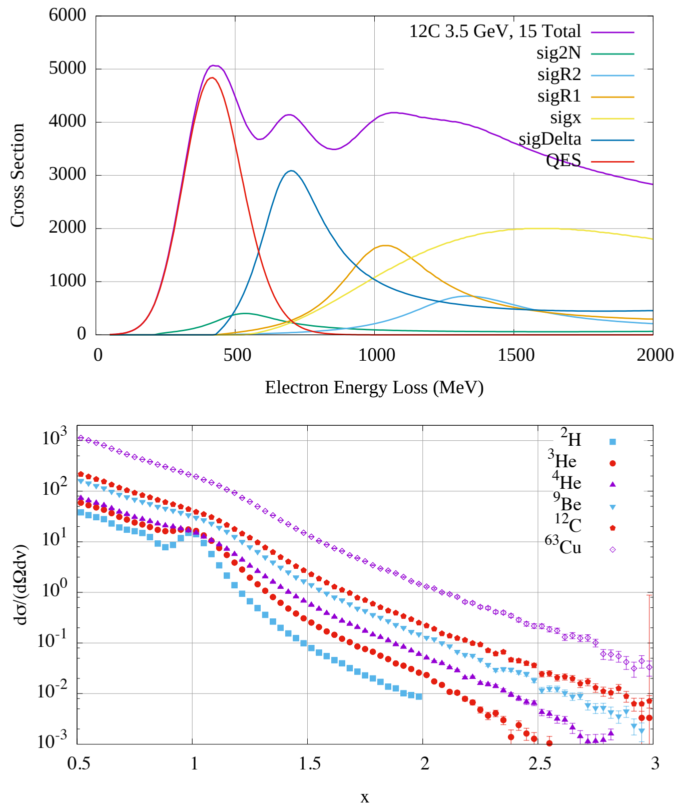

Figure 2. Top: Model calculation [17] of the various contributions to the inclusive electron cross section from ^{12}C at 3.5 GeV and 15°. Units are in millibarns/sr/MeV. Bottom: Cross sections from a recent Jefferson Lab experiment at 5.766 GeV and 18° on nuclei from ^{2}H to ^{64}Cu against x [2]. Units are 10^{-9}barns/sr/GeV.

$x < 1$. Energy loss less that that of the QEP corresponds to $x > 1$, forbidden to the free nucleon. Nucleons with momenta $k \leq k_F$ correlate with $x \lesssim 1.3$. Shown in the top of Figure 2, is a model [17] calculation of the spectrum of ^{12}C(e,e') against energy loss. The different contributions made separate: quasi-elastic scattering (QES), the excitation of the $\Delta(1232)$, and the two resonance regions (R1 and R2) and finally the dominant contribution at large energy loss and large momentum transfer, DIS (sigx). In this plot the quasi-elastic peak at an energy loss of about 400 MeV corresponding to $x = 1$. The bottom panel of Figure 2 hold recent inclusive cross section data from a Jefferson Lab experiment plotted against x for different nuclei. Note that the QEP broadens with increasing A and the high-k (large x) region scales - they have a common shape but a density, when divided by A, that increases with A. This scaling of the cross section is traceable to the two-body nature of SRC - at short distances nucleons in all nuclei experience the same potential and at large momenta all nuclei express the same behavior. The broadening of the momentum distribution with A both spreads out the QES strength but also pulls strength from the more inelastic channels under the peak at $x = 1$ and in heavy nuclei the peak is largely indistinguishable, a trait that grows with increasing momentum transfer due to the weaker dependence on Q^2 of the inelastic reactions.

4 SRC at Large x

It was first suggested by Frankfurt and Strikman [18, 19] that the relative contribution (probabilities) of SRC in nuclei relative to the deuteron would be quantified by the height of a plateau in the ratio $\frac{\sigma^A}{A} \Big/ \frac{\sigma^{2H}}{2}$ at $(1.4 < x < 2.0)$ where scattering from mean field nucleons is suppressed. In the impulse approximation the cross section can be represented as $\sigma(x, Q^2) = \sum_{j=2}^{A} A \frac{1}{j} a_j(A) \sigma_j(x, Q^2)$ where $\sigma_j(x, Q^2) = 0$ at $x > j$ and $a_j(A)$'s are proportional to the probabilities to find a nucleon in j–nucleon correlation. The above leads to the following scaling relations between scattering off the lightest nuclei (A=2) and heavier nuclei within the few nucleon correlation model, $\frac{2}{A}\sigma_A(x, Q^2)/\sigma_D(x, Q^2) = a_2(A) \mid_{1<x\leq 2}$ and $\frac{3}{A}\sigma_A(x, Q^2)/\sigma_{A=3}(x, Q^2) = a_3(A) \mid_{2<x\leq 3}$. σ_2 is chosen to be equal to the electron–deuteron cross section to define the normalization and then a_2 is closely related with the number of quasideutron pairs in the nucleus. Similarly, σ_3 is the cross section for the scattering from ^{3}He. Hence $a_2(A)$ is a measure of the number of 2N SRC in a nucleus A, relative to the deuteron. Similarly $a_3(A)$ is the number of 3N short correlations in the nucleus relative to the triton.

The advantage of taking ratios is that in the impulse approximation the elementary electron-nucleon cross section cancels as do any off–shell effects. As important is that FSI between the outgoing nucleons of the SRC is strongly dependent on the internucleon wave function at small distances, has only a very weak dependence on the nuclear environment and hence FSI are negligible in the ratios.

It was not until a comprehensive set of data from SLAC was analyzed that these plateaus were revealed [1] and found to be consistent with both the early predictions and realistic many-body calculations [8, 14, 20]. Recent data from Jefferson Lab experiment E-02-019 [2] can be seen in Figure 3. Data from Jefferson Lab [4] and BNL [3] have confirmed what theory has long understood: the dominant strength in this region of initial state momentum is due to $p - n$, isospin = 0 pairs [21]. Hence if the high-momentum contribution comes an n-p SRC at rest, then the ratios reveal the contribution of 2N-SRCs to the nuclear wave function, relative to the deuteron. An attempt to account for the motion of the pair was made in Ref. [2] following the prescription in [14] leading to the

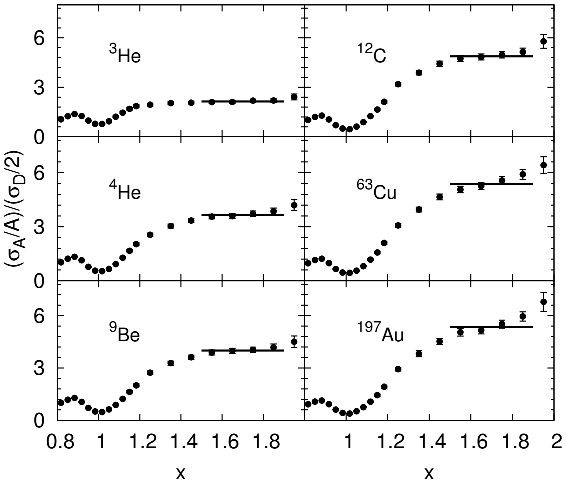

Figure 3. (LHS) Per-nucleon cross section ratios for 6 different nuclei in identical kinematics (E = 5.766 GeV and $\theta = 18^o$) from Jefferson Lab experiment E02019 [2].

introduction of a new measure, $R_{2N}(A, D)^*$ There it was argued that the c.m. motion spreads out the high-momentum tail resulting in an enhancement of the ratio in the plateau region on the order of 20%.

5 The EMC Effect

The unforseen observation [22] in the mid-1980's by the European Muon Collaboration (EMC) that the deep inelastic nuclear structure functions (from which the quark distributions, $q_i(x)$ can be extracted) $F^A_{1,2}(x, Q^2) \neq N \cdot F^n_{1,2}(x, Q^2) + Z \cdot F^p_{1,2}(x, Q^2)$ - the sum of proton and neutron contributions of the nucleus - triggered an avalanche of experimental and theoretical activity. Relevant reviews include Refs. [23–25]. The universal behavior of the EMC effect can be seen in Figure 4, i.e. the reduction in the strength of structure functions, (here) for carbon with respect to the deuteron for $0.35 < x < 0.7$. The magnitude of the depletion grows with A and is Q^2 independent. The physics explanations for the EMC effect can be organized into one of two groups. The first was developed using convolution models which included well founded nuclear effects - binding energies, detailed models of nucleon momentum distributions, and pion-exchange contributions. The nuclear dependence was examined [26] and found to be generally linear in the average nucleon density and with A. Many models of the EMC effect either implicitly or explicitly assume the size of the EMC effect scales with average nuclear density. Constraining the form of the nuclear dependence can confirm or rule out this assumption. The results from Jefferson

$^*a_2$ and $R_{2N}(A, D)$ are subtly different. The former represents the relative strength of the high-momentum tail while the latter suggests the relative number of pairs.

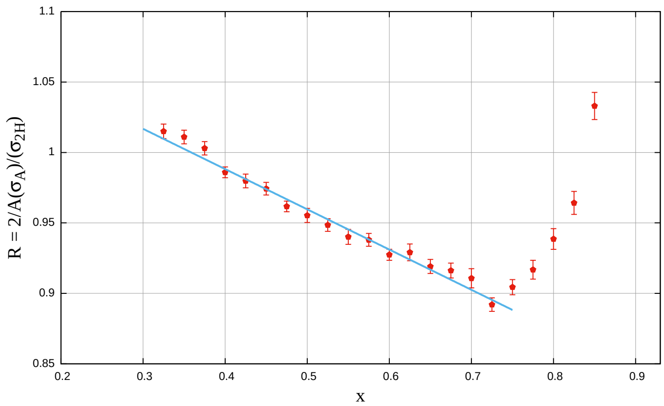

Figure 4. EMC ratio, $(\sigma_A/A)/\sigma_D/2)$, for carbon [27]. The slope, $|\frac{dR_{\text{EMC}}}{dx}|$, of the cross section ratios in the range $0.35 < x < 0.7$ quantifies the EMC effect. The solid line is a linear fit for $0.35 < x < 0.7$.

Lab experiment E03-103 [27] forced a reassessment as simple A- or density-dependent models for the EMC effect were found insufficient. See Figure 4 and Section 6.

6 Combining SRC and EMC

Two Jefferson Lab experiments that ran in 2004 provided the first opportunity to make the connection between cross section ratios in disparate kinematics: at $x > 1$ where the elementary process is QES from a moving, nearly free nucleon [2] and in DIS at $x < 1$ where the scattering is from the quarks that makes up the nucleon in the nucleus [27]. The qualitative observation that the magnitude of the EMC effect in nucleus A was linearly related to the SRC scale factor, $R_{2N}(A, D)$, was first made in [5] and the nuclear dependence of both $R_{2N}(A, D)$ and the magnitude of the EMC effect (the slope) $|dR_{\text{EMC}}/dx|$ was examined in detail in [28]. Figure 5 shows $R_{2N}(A, D)$ and $|dR_{\text{EMC}}/dx|$ plotted against the scaled average density, $\frac{A-1}{A}\rho(A)$ and where $\rho(A) = 3A/4\pi/R_e^3$ with $R_e = 5\langle r^2\rangle/3$ with$\langle r^2\rangle$ is the rms electron scattering radius [12]. Since the probed nucleon confronts the reduced density of (A-1) nucleons we scale the average nuclear density by (A-1)/A. The behavior of ^{9}Be is of special interest in that it differs from a dependence on the average density in both $R_{2N}(A, D)$ and $|dR_{\text{EMC}}/dx|$. ^{9}Be reveals a cluster character: 2 α particles surrounded by a single neutron with a *local* density similar to ^{4}He. Also ^{4}He is much lighter than ^{12}C, but has similar average density while ^{9}Be has much lower density than ^{12}C, but similar mass. Obviously, the average density can not be used to predict the EMC effect or the number of correlated pairs in a nucleus. We argued in [28] that "local" density most likely controls the nuclear responses discussed here.

This is in contrast with the conclusion of the authors of [5, 6] who argued that both processes probe high-momentum nucleons and the virtuality of the process is responsible for the connection between $R_{2N}(A, D)$ and $|dR_{\mathrm{EMC}}/dx|$. Much theoretical work remains to be done if this connection is to be understood.

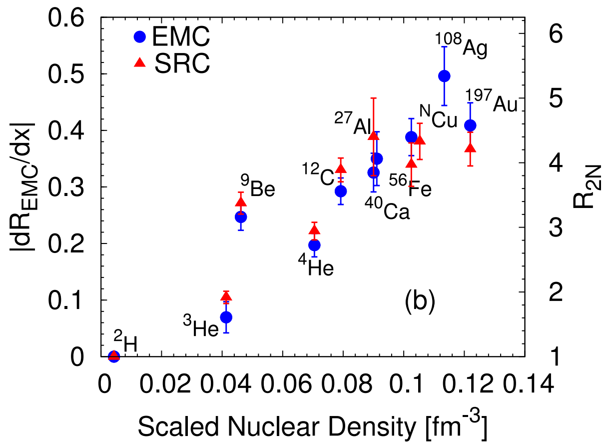

Figure 5. $\left|\frac{dR_{\mathrm{EMC}}}{dx}\right|$ (left hand axis) and $R_{2N}(A, D)$ (right hand axis) both against scaled average density $\frac{A-1}{A}\rho(r)$. Consider the anomalous behavior of ^{9}Be, ^{4}He and ^{12}C which suggests that the average nuclear density is not a proxy for either the EMC effect or SRC.

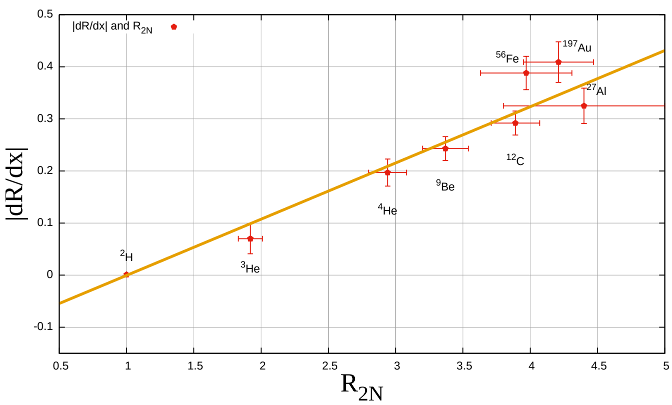

Figure 6. $\left|\frac{dR_{\mathrm{EMC}}}{dx}\right|$ versus $R_{2N}(A, D)$. The straight line is a fit that is constrained to go through the contrived ^{2}H datapoint at (1,0), required as its EMC slope would be 0 and the number of pn pairs relative to itself is 1.

7 Future Studies

Jefferson Lab has planned a series of experiment will provide greater insight into the role of SRC. In 2017 ^{3}He and ^{3}H [29] will be studied in the large x region. These mirror nuclei will allow a test of the isopsin dependence in the SRC region. In their ratios we find two extreme outcomes. The first is if the SRC is dominated by pn pairs we would obtain: $\frac{\sigma_{^3He}/3}{\sigma_{^3H}/3} = \frac{(2pn + 1nn)/3}{(2pn + 1pp)/3} = 1.0$ as $1pp$ and $1nn$ would not contribute. If all pairs contribute to the SRC regions at $x > 1$, we expect $\frac{\sigma_{^3He}/3}{\sigma_{^3H}/3} = \frac{(2\sigma_p + 1\sigma_n)/3}{(1\sigma_p + 2\sigma_n)/3}$ and as $\sigma_p \approx 3\sigma_n$ and $\frac{\sigma_{^3He}/3}{\sigma_{^3H}/3} \to 1$. This ratio can be measured to 4% making a determination of the isospin dependence possible. In addition the 3-body systems are theoretically manageable allowing tests of cross sections arising from ab-initio calculations as well as of FSIs. In 2018/19 companion experiments, E12-06-105 [30] and E12-10-008 [31], will run. The first is designed to push studies of inclusive scattering from nuclei at $x > 1$ with a range of momentum transfer that will extend from the quasi-elastic region at moderate Q^2 and very large x to study 2 and 3N SRC to very large Q^2 and $1 < x < 1.2$ where the cross section is dominated by DIS. This will allow us to search for the effects of short distance behavior and possibly exotic components when scattering from quarks. The second experiment will push the study of the EMC effect to higher Q^2 values. Both will make use of electrons energies as high as 11 GeV from the upgraded accelerator. We seek to employ not only the very light targets but others that will help unravel the role of density and isospin in inclusive reactions on both sides of the QEP. Potential targets include ^{3}He, ^{4}He, ^{6}Li, ^{7}Li, ^{9}Be, ^{10}B, ^{11}B, ^{12}C, ^{40}Ca, ^{48}Ca, and ^{63}Cu. Neutron rich nuclei are attractive as the protons are more likely that neutrons to be correlated in np pairs [32]. Taking the SRC and EMC relationship at face value would imply that the u-quark and d-quark distributions would be modified differently.

8 Conclusion

Many years of effort has generated a significant body of work illuminating the role of short range correlations in nuclei. The ratios of per nucleon cross section of heavy to light nuclei has the potential to provide information about 2N and 3N correlations, their strength and isospin character. The connection between SRC and the EMC effect has been established. Much is left to do.

References

[1] L.L. Frankfurt, M.I. Strikman, D.B. Day, and M. Sargsian, *Phys. Rev. C* **48** (1993) 2451-2461.

[2] N. Fomin et al., *Phys. Rev. Lett.* **108** (2012) 092502.

[3] E. Piasetzky, M. Sargsian, L. Frankfurt, M. Strikman, and J.W. Watson, *Phys. Rev. Lett.* **97** (2006) 162504.

[4] R. Subedi et al., *Science* **320** (2008) 1476-1478.

[5] L.B. Weinstein, E. Piasetzky, D.W. Higinbotham, J. Gomez, O. Hen, and R. Shneor, *Phys. Rev. Lett.* **106** (2011) 052301.

[6] O. Hen, E. Piasetzky, and L.B. Weinstein, *Phys. Rev. C* **85** (2012) 047301.

[7] A.N. Antonov, P.E. Hodgson, and I.Zh. Petkov, *Nucleon Correlations in Nuclei*, (Springer, 1993).

[8] M. Alvioli, C.C. degli Atti, L.P. Kaptari, C. B. Mezzetti, and H. Morita, *Int. J. Mod. Phys. E* **22** (2013) 1330021.

[9] J. Arrington, D.W. Higinbotham, G. Rosner, and M. Sargsian, *Prog. Part. Nucl. Phys.* **67** (2012) 898-938.

[10] V.R. Pandharipande, I. Sick, and P.K.A. deWitt Huberts, *Rev. Mod. Phys.* **69** (1997) 981-991.

[11] H. Muther and I. Sick, *Phys. Rev. C* **70** (2004) 041301.

[12] H. De Vries, C.W. De Jager, and C. De Vries, *Atomic Data and Nuclear Data Tables* **36** (1987) 495-536.

[13] L. Lapikas, *Nucl. Phys. A* **553** (1993) 297-308.

[14] C.C. degli Atti and S. Simula, *Phys. Rev. C* **53** (1996) (1996) 1689.

[15] S. Frullani and J. Mougey, *Adv. Nucl. Phys.* **14** (1984) 1.

[16] W. Czyz and K. Gottfried, *Ann. Phys.* **21** (1963) 47-71.

[17] J.W. Lightbody and J.S. O'Connell, *Computers in Physics* **2** (1988) 57-54.

[18] L.L. Frankfurt and M.I. Strikman, *Phys. Rep.* **76** (1981) 215-347.

[19] L.L. Frankfurt and M.I. Strikman, *Phys. Rep.* **160** (1988) 235-427.

[20] C.C. degli Atti, S. Simula, L.L. Frankfurt, and M.I. Strikman, *Phys. Rev. C* **44** (1991) R7-R11.

[21] O. Benhar, A. Fabrocini, and S. Fantoni, *Nucl. Phys. A* **505** (1989) 267-299.

[22] J.J. Aubert et al., *Phys. Lett. B* **123** (1983) 275-278.

[23] D.F. Geesaman, K. Saito, and A.W. Thomas, *Ann. Rev. Nucl. Part. Sci.* **45** (1995) 337-390.

[24] P.R. Norton, *Rep. Prog. Phys.* **66** (2003) 1253-1297.

[25] K. Rith, *Subnucl. Ser.* **51** (2015) 431-449.

[26] J. Gomez et al., *Phys. Rev. D* **49** (1994) 4348-4372.

[27] J. Seely et al., *Phys. Rev. Lett.* **103** (2009) 202301.

[28] J. Arrington, A. Daniel, D. Day, N. Fomin, D. Gaskell, and P. Solvignon, *Phys. Rev. C* **86** (2012) 065204.

[29] P. Solvignon-Slifer, J. Arrington, D. Day, and D. Higinbotham, Precision measurement of the isospin dependence in the 2N and 3N short range correlation region, Jefferson Lab Experiment E12-11-112, 2011.

[30] J. Arrington and D. Day, Inclusive scattering from nuclei at x $>$ 1 in the quasielastic and deeply inelastic regimes, Jefferson Lab Experiment No. E12-06-105, unpublished, 2006.

[31] D. Gaskell, J. Arrington, and A. Daniel, Detailed studies of the nuclear dependence of F_2 in light nuclei, Jeffersson Lab experiment E12-10-008, unpublished, 2010.

[32] O. Hen et al., *Science* **346** (2014) 614-617.